LA-UR- 09-00212

Approved for public release; distribution is unlimited.

Title:	A Dynamic Chamber System Coupled With a Tunable Diode Laser for Online Measurements of Delta-13C, Delta-18O, and Efflux Rate of Soil Respired ~~Carbon Dioxide~~ CO_2
Author(s):	Heath H. Powers Nate G. McDowell David T. Hanson John E. Hunt
Intended for:	Submission to the journal Global Change Biology

Los Alamos
NATIONAL LABORATORY
EST. 1943

Form 836 (7/06)

A dynamic soil chamber system coupled with a tunable diode laser for online measurements of $\delta^{13}C$, $\delta^{18}O$, and efflux rate of soil respired CO_2

Running Title: Soil chamber coupled with TDL reveals high frequency response to pulse watering.

Heath H. Powers, *Corresponding author*
Earth and Environmental Sciences Division
MS-J495
Los Alamos National Laboratory
Los Alamos, NM 87545, USA
hpowers@lanl.gov, 505-606-0795

John E. Hunt
Landcare Research
Global Change Processes
PO Box 40
Lincoln 7640, New Zealand,

David T. Hanson
University of New Mexico
Department of Biology
167 Castetter Hall
Albuquerque, NM 87131, USA

Nate G. McDowell
Earth and Environmental Sciences Division
MS-J495
Los Alamos National Laboratory
Los Alamos, NM 87545, USA

For submittal to *Global Change Biology*

January 6, 2009

Keywords: soil respiration, delta 13C, delta 18O, tunable diode laser, soil chamber, stable isotope

Abstract

High frequency observations of the stable isotopic composition of CO_2 effluxes from soil have been sparse due in part to measurement challenges. We developed an open-system method that utilizes a flow-through chamber coupled to a tunable diode laser (*TDL*) to quantify the rate of soil CO_2 efflux and its $\delta^{13}C$ and $\delta^{18}O$ signatures. We tested the method first in the laboratory using an artificial soil test column and then in a semi-arid woodland. We found that CO_2 efflux rates of 1.2 to 7.3 μmol m^{-2} s^{-1} measured by the chamber-*TDL* system gave similar results to measurements made using the chamber and an infrared gas analyzer (*IRGA*) (R^2=0.99) and compared well to efflux rates generated from the artificial test column (R^2=0.94). Measured $\delta^{13}C$ and $\delta^{18}O$ of CO_2 efflux from the test column were not significantly different from measurements of gas inside of the test column across all efflux rates ($p > 0.05$) after accounting for diffusive enrichment. Isotopic differences between chamber measurements and values from CO_2 gas introduced into the test column resulted primarily from diffusion of atmospheric CO_2 into the test column and pressure artifacts from the chamber. Field measurements during drought demonstrated a strong dependency of CO_2 efflux and isotopic composition on soil water content. Addition of water to the soil beneath the chamber resulted in average changes of +6.9 μmol m^{-2} s^{-1}, -5.0‰, and –55.0‰ for soil CO_2 efflux, $\delta^{13}C$ and $\delta^{18}O$, respectively, within 25 minutes of water addition. The soil chamber coupled with the *TDL* was found to be an effective method for capturing high-resolution soil CO_2 efflux and its stable isotopic composition.

Introduction

Atmospheric measurements of CO_2 mole fraction have allowed scientists to determine that globally about half of anthropogenically emitted CO_2 stays in the atmosphere and the rest is absorbed by the biosphere (Battle et al. 2000). The isotopic composition of the carbon and

69 oxygen ($\delta^{13}C$ and $\delta^{18}O$ respectively) of CO_2 in the atmosphere reflect strong fractionation by
70 terrestrial ecosystems dominated by C_3 and to a lesser extent C_4 plants (Bender 1971).
71 Therefore, the isotopic signatures of terrestrial respiratory effluxes are a valuable tracer of CO_2
72 movement through terrestrial ecosystems (Miller et al. 2003) and provide an opportunity to
73 partition oceanic and terrestrial carbon fixation (Ciais et al. 1995). However, models that
74 partition sources and sinks of carbon based on constant values of terrestrial isotopic fractionation
75 during respiration may give incorrect results (Fung et al. 1997, Randerson et al. 2002b). Soil CO_2
76 efflux plays a major role in global carbon cycling and in the isotopic content of atmospheric
77 CO_2. Annually, it is estimated that 68 Gt of CO_2 evolves from the soil (Raich & Schlesinger
78 1992), more than 10 times the amount emitted anthropogenically through fossil fuel combustion
79 (Randerson et al. 2002a). Soil respired CO_2 is produced from heterotrophic decomposition of
80 organic matter and from autotrophic respiration of plant roots in the rhizosphere (Law et al.
81 1999). Soil respired $\delta^{13}C$ ($\delta^{13}C_R$) and $\delta^{18}O$ ($\delta^{18}O_R$) is variable but the mechanisms regulating
82 these signatures are poorly understood (Cerling 1984, Farquhar et al. 1993, Ehleringer et al.
83 2000).

84 Several studies have utilized chamber-based measurements of bulk soil CO_2 efflux to
85 quantify ecosystem carbon cycling but far fewer have incorporated measurements of stable
86 isotopes of respired CO_2. Of the studies that incorporated these measurements, several chamber
87 types were used but all involved periodically collecting gas samples and taking them for post
88 analysis with a mass spectrometer (Miller *et al.* 1999, Ekblad & Hogberg 2000, McDowell *et al.*
89 2004). Although these earlier studies were able to capture *in situ* measurements of the isotopic
90 composition of soil CO_2 efflux, they were unable to conduct experiments with high temporal
91 resolution. In these experiments, the frequency of sample collection was inherently limited by

92 the time and effort required by flask collection and off-line analysis by a mass spectrometer. An
93 additional complication is that chamber-based samples of soil respired CO_2 are difficult to
94 collect without adversely affecting the soil efflux and isotopic composition. This is partly due to
95 the mass flow of soil gas that is drawn into the chamber headspace in order to replace the volume
96 removed by the sample (Rayment & Jarvis 1997). The replacement gas can either come from the
97 soil, which generally has a high CO_2 concentration ($[CO_2]$) and is enriched in heavier isotopes
98 (Cerling et al. 1991), or from the atmosphere, which dilutes the soil gas in the chamber and again
99 alters the isotopic signature in the chamber.
100 Two system configurations can be employed to measure fluxes and isotopic composition
101 of soil respired CO_2. Open or flow-through soil chambers have a continuous flow of air through
102 the chamber headspace, an inlet for incoming air, an outlet that exhausts gas from the chamber,
103 and an opening to the soil surface. Information about $[CO_2]$, $\delta^{13}C_R$ and $\delta^{18}O_R$ (δ_R collectively)
104 are calculated from differences of measurements of the air entering and exiting the chamber.
105 Closed chambers have an opening to the soil but are otherwise closed to the atmosphere; gas
106 exiting the chamber is recirculated into the chamber headspace and determinations of efflux rate
107 and isotopic composition are derived based upon the buildup of CO_2 over time within the
108 chamber and the corresponding changes in isotopic values. Open chambers are known to be
109 susceptible to pressure differentials between the inside of the chamber and ambient pressure due
110 to air either being blown or drawn through the chamber (Davidson *et al.* 2002, Widen &
111 Lindroth 2003). Differences in pressure as little as 1 Pa have been shown to affect efflux
112 measurements by inducing mass flow of CO_2 either into or out of the soil (Fang & Moncrieff
113 1996). Pressure differences of less than 0.1 Pa are needed to minimize impacts on soil CO_2
114 efflux measurements (Fang & Moncrieff 1996). Since closed chambers recirculate gas through

115 their headspace, they keep the entire volume of gas in the system contained and as such they are
116 a constant volume system. If a sub-sample is drawn from a closed chamber, the pressure is
117 decreased proportionally to the volume of the sample removed. Generally, the pressure is
118 subsequently equalized by mass movement of gas from the soil into the chamber or from the
119 atmosphere through a pressure-equalizing vent (Lund *et al.* 1999). In contrast, open chambers
120 are not constant volume systems since gas is constantly introduced into the inlet and exhausted
121 from the outlet.

122 An advantage of open chambers for isotopic measurements is that sub-samples can be
123 collected from the inlet and exhaust of the chamber without altering the pressure inside of the
124 chamber. This allows for determination of $\delta^{13}C$ and $\delta^{18}O$ of CO_2 emitted from soil using the
125 "on-line" approach of Evans et al. (1986) (equation 2). This technique lends itself well to high
126 frequency analysis using tunable diode laser (*TDL*) absorption spectroscopy for measurements of
127 CO_2 entering and exiting the soil chamber. The *TDL* uses a laser that can vary its frequency in
128 order to match the absorption frequency of specific isotopologues and scan the breadth of the
129 absorbance feature (Bowling et al. 2003). This is done for all of the isotopologues of interest
130 (e.g. $^{13}C^{16}O_2$, $^{12}C^{16}O_2$, $^{12}C^{18}O^{16}O$) with high frequency so mole fractions of each species can be
131 found. The particular instrument used in this study (TGA100A, Campbell Scientific) has a scan
132 rate of 500Hz with data output averaged to 10Hz for high frequency measurements, although
133 typically measurements are averaged for 10 – 15 seconds for improved precision. *TDL*
134 measurements have become increasingly important in ecological studies because they allow
135 large numbers of measurements to be collected continuously and they simultaneously measure
136 [CO_2] and stable isotopic composition (Bowling et al. 2003, Griffis et al. 2005, McDowell et al.
137 2008).

138 Here, we explore the use of a *TDL* coupled to a dynamic flow-through chamber system
139 modified from Fang and Moncrieff (1996) for measuring soil CO_2 efflux and determining $\delta^{13}C_R$
140 and $\delta^{18}O_R$ of soil respiration at high temporal frequency. We used a *TDL* for sampling the inlet
141 and outlet of the chamber in order to produce these measurements at 2 minute intervals, a
142 frequency sufficient to capture rapid, transient shifts in respiration and δ_R value. We assessed the
143 accuracy and precision of this chamber system using an artificial test column with known efflux
144 rates and isotopic composition. Additionally, we field tested the chamber to determine the ability
145 of the system to capture dynamic, transient events associated with pulse wetting of soils.
146
147 **Theory**
148 Soil CO_2 respiration strongly controls near-surface [CO_2] and its stable isotopic
149 composition. In C_3 dominated ecosystems, plant root and soil microbial respiration generates
150 $\delta^{13}C_R$ values from -23‰ to -30‰ (Ehleringer et al. 2000). The large surface area of soils and the
151 high [CO_2] contained within them lend a significant contribution to the $\delta^{13}C$ of the atmosphere
152 near the surface.
153 Respiration of plant roots and soil microbes releases CO_2 with a particular $\delta^{13}C$ and $\delta^{18}O$
154 into the soil. The soil matrix through which CO_2 molecules diffuse causes a change in the $\delta^{13}C$
155 and $\delta^{18}O$ relative to their source due to kinetic fractionation , estimated to be 4.4‰ for $\delta^{13}C$ and
156 8.8‰ for $\delta^{18}O$ (Cerling et al. 1991). Under steady state conditions, CO_2 within the soil is
157 isotopically enriched while gas leaving the soil surface has the same isotopic composition as the
158 source emitting CO_2 into the soil (Amundson et al. 1998).
159 Liquid water in soils has an effect on the respired $\delta^{18}O$ value of CO_2 in the soil. CO_2 that
160 is in contact with water exchanges oxygen atoms with water molecules. This causes the $\delta^{18}O$ of

161 CO_2 to be influenced by the $\delta^{18}O$ of the water. The degree of influence depends on a number of
162 factors including the amount of time the CO_2 is in contact with the water, temperature, and the
163 presence of catalyzing enzymes such as carbonic anhydrase (Tans 1998).

164 Net soil CO_2 efflux is determined by the mass balance equation modified from Ball
165 (1999):

166 $$r = \frac{u_o(c_i - c_o)}{s} - E \qquad (1)$$

167 where r is net soil CO_2 efflux ($\mu mol\ CO_2\ m^{-2}\ s^{-1}$), u_o is flow rate out of the chamber ($\mu mol\ s^{-1}$), c_i
168 is the mole fraction of CO_2 entering the chamber ($\mu mol\ mol^{-1}$), c_o is the mole fraction of CO_2
169 going out of the chamber ($\mu mol\ mol^{-1}$), s is the surface area of soil being measured by the
170 chamber (m^2), and E is the efflux rate of water leaving the soil ($\mu mol\ H_2O\ m^{-2}\ s^{-1}$). When there is
171 a large amount of water evaporating from the soil, the E term can be a significant contribution to
172 the mass flow of air exiting the chamber, effectively diluting the mass flow of CO_2 from the
173 chamber.

174 The equation for the soil evaporative term is modified from Ball (1989):

175 $$E = \frac{F(w_o - w_i)}{Sm^2(1000 - w_i) \times 10^6} \qquad (2)$$

176 Where F is the mass flow rate in μmol s^{-1} of gas leaving the chamber, w_o and w_i are the exiting
177 and entering water vapor, respectively, in mmol H_2O per mole of air.

178 A mass balance equation is used to determine the respired $\delta^{13}C$ and $\delta^{18}O$ based on the
179 difference in inlet and outlet δ values. The equation below is modified from a leaf chamber
180 (Evans et al. 1986) to apply the equation to a dynamic open soil chamber:
181

182 $$\delta_R = \frac{c_o \delta_o - c_i \delta_i}{c_o - c_i} \quad (3)$$

183 where δ_R is the isotopic value of CO_2 respired from the soil relative to the isotopic standards
184 VPDB for $\delta^{13}C$ and VSMOW for $\delta^{18}O$, δ_o is the delta value of the chamber outlet and δ_i is the
185 delta value of the chamber inlet.
186
187 **Methods**
188 *Chamber Design*
189 The soil chamber used in this study is a dynamic flow-through chamber modified from
190 Fang and Moncrieff (1996). The chamber was constructed from 3 mm polycarbonate and was a
191 rectangular design with an internal volume of 2.65 L (Figure 1). The inlet and outlet are located
192 on either side of the chamber with a metal mesh placed in front of both the inlet an outlet to help
193 reduce pressure waves from crossing the chamber. A slowly turning three-bladed fan (18 RPM)
194 was used in the top of the chamber above the soil gas inlet to aid in mixing. The chamber
195 bottom was circular with a diameter of 142 mm and a surface area of 15.8×10^{-3} m^2. The bottom
196 edge of the chamber protruded 30 mm from the lower surface and fit into a water-sealed metal
197 soil collar that was driven into the soil or test column medium. The chamber was equipped with
198 a thermocouple for measuring chamber headspace temperature, a port with an attached tube for
199 connection to a differential pressure transducer, and a circular, perforated manifold placed over
200 the bottom opening attached to an external tube for water delivery (watering experiments only).
201
202 *Chamber operation*
203 The flow rate through the chamber was controlled with a mass flow controller (*MFC*,
204 FMA-A2408, Omega Engineering) connected to a diaphragm vacuum pump and attached to the

chamber outlet in order to draw gas through the chamber. In order to minimize pressure differentials induced by restriction of the chamber inlet, a compressed gas cylinder of medical grade air was attached to the chamber inlet and incoming flow was regulated with a mass flow controller in order to balance it with the rate that air was drawn from the chamber (Figure 1). Prior to all measurements, the bottom of the chamber was sealed with closed-cell foam and the chamber flow-rate was set with the outlet flow controller to the desired flow-through rate (between 0.2 and 1 L min^{-1}, depending on the experiment). A differential pressure transducer (PX653, Omega Engineering) was connected to measure the pressure difference between the inside of the chamber and the ambient air. The flow rate from the air cylinder was then adjusted in order to bring the pressure differential to within ± 0.05 Pa, the resolution limit of the pressure transducer. After balancing the pressure of the chamber, the foam was removed from the bottom of the chamber and the chamber was placed on the collar for measurements.

A tee fitting (Figure 1) was placed at both the chamber inlet and outlet to allow sub-sampling by the *TDL* and an infra-red gas analyzer (*IRGA*, LI-840, Li-Cor Biosciences) for determination of chamber CO_2 efflux, $\delta^{13}C_R$ and $\delta^{18}O_R$. The tee for the outlet first entered the *IRGA* for [CO_2] analysis, then passed through a critical flow orifice (restricting flow to 200 mL min^{-1}) and into the *TDL* for [CO_2], $\delta^{13}C$, and $\delta^{18}O$ analysis before being exhausted by the vacuum pump. The sub-sample from the chamber's inlet passed directly through the critical flow orifice and to the *TDL* for the same analyses of air entering the soil chamber. The venting tee (Figure 1) is used to maintain the pressure of the soil chamber at atmospheric pressure.

Artificial test column

227 A test column was designed to produce a known CO_2 efflux rate with a known isotopic
228 composition for testing the soil chamber (Figure 2). The cylindrical column was constructed of
229 aluminum with a diameter of 1 m and height of 1.3 m. The bottom was sealed with sheet
230 aluminum and the top had a perforated stainless steel grate (holes are 3.2 mm in diameter, 22.3
231 holes per cm^2) fitted 10 cm from the top edge. The interior CO_2 delivery manifold of the test
232 column was made from a 1.5 m length of copper tubing (1.3 mm ID) with small perforations
233 approximately 60 mm apart. A similar manifold was constructed from 0.4 m of copper tubing,
234 either end of which was connected to an IRGA (Li- 820, Li-Cor Biosciences) in a closed loop for
235 sampling CO_2 mole fractions in the interior of the column. A slowly rotating mixer (12 RPM)
236 was placed in the bottom of the column above the CO_2 delivery manifold to aid in homogenizing
237 the interior air. An 80 mm layer of dry glass beads (3 mm diameter) was used as the substitute
238 for soil, this was held up by a porous nylon fabric and placed on a perforated metal grate at the
239 bottom of the glass beads in the test column.
240 Efflux from the test column was generated by creating a large CO_2 gradient between the
241 interior of the column and ambient air, causing CO_2 to diffuse out the top of the column. CO_2
242 efflux rates from the test column were generated by maintaining a constant [CO_2] inside the
243 column; efflux was determined by measuring the amount of pure CO_2 gas that was needed to
244 maintain the [CO_2]. A mass flow controller (FMA-2402, Omega Engineering, 20 mL min^{-1}
245 maximum) was used to regulate the flow of CO_2 into the column interspace. A data logger (CR-
246 1000, Campbell Scientific) was programmed with a feedback algorithm, based on measurements
247 of the [CO_2] in the test column,, regulated the delivery of CO_2 needed to maintain the target
248 concentration . Commands were sent to the mass flow controller every second and flow data
249 was recorded and averaged over 5 minute intervals to determine efflux from the test column.

To determine $\delta^{13}C_R$ and $\delta^{18}O_R$ from test column efflux, *TDL* measurements were made from air drawn from the interior of the test column. In order to bring a gas sample of suitable concentration for *TDL* sampling, mass flow controllers were used to mix test column gas with CO_2 free air to produce a sample stream with a $[CO_2]$ of ~400 μmol mol^{-1}. These values were assumed to be isotopically enriched due to kinetic fractionation and were converted to δ_R values were by subtracting 4.4‰ for $\delta^{13}C$ and 8.8% for $\delta^{18}O$, giving known values of $\delta^{13}C_R$ = 39.0‰ ± 0.3‰ and $\delta^{18}O_R$ = 9.7‰ ± 0.3‰.

Soil Chamber Operation

Prior to testing, a soil collar was placed in the test column, the test column was sealed and all of the CO_2 was removed using a soda lime scrubber. Testing began by first bringing the interior air of the test column to a steady-state target $[CO_2]$ as determined by the *IRGA*. The chamber was then placed on the collar for efflux measurement and the flow rate through the chamber was chosen as either 300 or 500 mL min^{-1}. These rates were chosen to optimize the chamber headspace $[CO_2]$ by maximizing the difference between c_o and c_i but remaining within the calibrated range of the *TDL* (between 300 and 650 μmol mol^{-1}). Chamber measurements of $[CO_2]$ were made using both the *TDL* and *IRGA* to independently determine efflux rates for comparison of the *TDL*–based measurement to the traditional *IRGA*-based measurement. Since the *IRGA* only measured the chamber outlet, a predetermined value for $[CO_2]$ from the medical air cylinder was used as the inlet value in *IRGA* based efflux calculations. Chamber measurements of the test column were conducted at multiple column CO_2 efflux rates. The test column was allowed to equilibrate at each efflux rate for a minimum of 4 hours before

measurements were recorded, and chamber measurements were conducted for a minimum of 6 hours.

TDL Absorption Spectroscopy Measurements

The *TDL* sampled both the inlet and the outlet of the soil chamber at a frequency of one measurement cycle every two minutes. Each cycle consisted of measurements of two calibration standards (high standard: $[CO_2]$ = 558.94 μmol mol^{-1}, $\delta^{13}C$ = -30.52‰, $\delta^{18}O$ = 0.68‰; low standard: $[CO_2]$ = 339.89 μmol mol^{-1}, $\delta^{13}C$ = -30.60‰, $\delta^{18}O$ = -0.33‰) followed by measurements of samples from the chamber inlet and outlet. A multiport manifold was used to direct flow from each inlet into the sample path of the *TDL* for a total of 30 seconds with the last 15 seconds averaged for each measurement. Determinations of mole fractions for $^{12}C^{16}O_2$, $^{13}C^{16}O_2$, and $^{12}C^{18}O^{16}O$ were corrected during post-processing by applying a linear correction to each measurement cycle derived from the difference between measured and actual values of the calibration standards (see Bowling et al. 2005). Corrected isotopologue values were converted into isotopic compositions and expressed relative to known standards (VPDB, Vienna Pee Dee Belemnite for $\delta^{13}C$ and VSMOW, Vienna Standard Mean Ocean Water for $\delta^{18}O$). For the $[CO_2]$ values used in equations (1) and (3), measured isotopologues values were summed and a fraction for all other non-measured isotopologues was added (Barbour et al. 2007).

Soil Watering Experiment

The field tests were conducted using the piñon-juniper woodland located outside of our *TDL* facility at Los Alamos National Laboratory in northern New Mexico, USA. The soil chamber was configured in the same manner as for the test column. One day prior to

295 measurements, collars were placed in the soil to allow soil CO_2 efflux to stabilize from
296 disturbance from placement (Law et al. 1999). After adjusting chamber flow-rate and equalizing
297 the chamber pressure with the atmosphere, the chamber was placed on the collar and sealed with
298 water. Data for the chamber inlet and outlet [CO_2], $\delta^{13}C$ and $\delta^{18}O$ were collected every two
299 minutes with the *TDL*, chamber outlet [CO_2] and water vapor were collected at 1Hz with the
300 *IRGA* and logged with the data logger. The [CO_2] in the chamber headspace was allowed to
301 stabilize and data collected for at least 30 minutes prior to water addition. After the initial
302 stabilization and measurement period, a simulated 50 mm rain event was added, without
303 removing the soil collar, through the watering manifold to evenly wet the soil. Water addition
304 was done over approximately a 4 minute period to prevent any water from standing within the
305 soil collar. Data was collected from the soil chamber before, during and after the watering event.
306
307 **Results**
308 Carbon dioxide efflux rates generated in the test column were calculated using [CO_2]
309 measurements from both the *TDL* and *IRGA* for comparison. Both methods yielded comparable
310 data (Figure 3, linear regression $R^2 = 0.99$, $p<0.0001$). The TDL-chamber measurements of
311 efflux rates from the column were in good agreement with the column efflux rates (Figure 4).
312 The 1:1 line (shown) shows that across all efflux rates and for both the 300 and 500 mL min^{-1}
313 chamber flow-through rates there is considerable agreement between logger-based efflux
314 measurements and TDL-based efflux measurements (Table 1). For both chamber flow-through
315 rates, the chamber measurements of column CO_2 effluxes were not significantly different from
316 known values ($p=0.54$). There was a linear relationship across the data (slope = 0.95, $R^2=0.94$)
317 for all data and for the 300 and 500 mL flow rates separately (slope = 0.68, $R^2=0.93$ and slope =

318 0.94 and R^2= 0.95 respectively). Both show no significant difference in measured efflux from
319 test column efflux (p=0.35 and p=0.87 for the 300 and 500 mL min^{-1} flow rates, respectively).
320 For all flow rates and efflux rates on the test column, $\delta^{13}C_R$ and $\delta^{18}O_R$ measurements
321 from the chamber were not significantly different than the expected values (Table 1, Figure 5).
322 Likewise, individual comparisons by flow rate and within $\delta^{13}C_R$ and $\delta^{18}O_R$ did not show any
323 significant differences between expected values and measurements from the chamber (Table 1).
324 Field measurements showed an average efflux rate of 0.3 ± 0.05 μmol CO_2 m^{-2} s^{-1} for dry
325 soils prior to watering (Table 2, Figure 6). Addition of a 50 mm rain event to the soil caused a
326 24-fold increase to 7.2 ± 0.5μmol m^{-2} s^{-1}. Isotopic values of dry soil respiration had a value of
327 $\delta^{13}C_R$ = -20.6 ± 3.0‰ and $\delta^{18}O_R$ = 80.3 ± 7.7‰. The addition of water changed $\delta^{13}C_R$ by -5.0‰
328 to -25.6 ± 0.7‰ and $\delta^{18}O_R$ by -55.0‰ to 25.3 ± 1.2‰. The addition of water increased the
329 gravimetric water content of the dry soil (0 – 100 mm depth) by 5-fold, from an average of 2.8%
330 to 14.2% and changed the $\delta^{18}O_R$ from 2.8 ± 1.7‰ to -8.3 ± 1.8‰.
331
332 **Discussion**
333 *Test Column*
334 Soil [CO_2] is elevated above atmospheric [CO_2] by autotrophic respiration (roots) and
335 heterotrophic respiration (microorganisms), creating a gradient that drives CO_2 diffusion from
336 the soil. Steady-state CO_2 efflux is achieved when CO_2 is lost to the atmosphere at the same rate
337 that it is introduced to the soil through respiration. We designed a test column to mimic CO_2
338 effluxes from a dry, coarse soil. The test column simulated this by regulating the [CO_2] of the
339 volume underneath the soil substrate: as CO_2 was lost from the system through surface efflux, an
340 equivalent amount was added to the column to maintain stable [CO_2] and by extension, a steady

341 state CO_2 efflux rate. The ability to precisely monitor the amount of CO_2 needed to maintain the
342 internal [CO_2] gives an accurate method for determining the efflux from the test column.
343 The soil chamber used in this study provided accurate measurements of soil CO_2 efflux,
344 $\delta^{13}C_R$, and $\delta^{18}O_R$ (Figures 5 and 6). Since *TDL* absorbance spectroscopy is a new technology
345 and has not been used in the past for determining soil chamber-based efflux measurements, we
346 verified the accuracy of the CO_2 efflux with simultaneous measurements with a previously tested
347 *IRGA*. Both methods fall along the 1:1 line (Figure 3) and have comparable degrees of variation.
348 Since the *TDL* was on a 30 second measurement cycle, there is a 30 second lag between
349 measurements of the chamber inlet and outlet gases. Although this could be problematic if there
350 were significant and rapid changes in inlet [CO_2], however, the use of a compress gas cylinder
351 avoids this problem by maintaining a constant isotope and concentration source. This problem
352 can also be ameliorated with the use of a buffer volume to stabilize inlet gas CO_2 fluctuations.
353 Measurements of the inlet [CO_2] and isotopic composition by *TDL* showed very little variance
354 (standard deviation = 0.18 $\mu mol\ mol^{-1}$) and the flux measurements from both instruments
355 corresponded closely (Figure 3).
356 We verified the accuracy of soil efflux measurements with this chamber system by
357 comparing chamber-based efflux measurements with effluxes generated by the test column. By
358 using glass beads for the diffusive medium, we introduce no potential source of carbon to affect
359 test column effluxes or isotopic values. Secondly, since the glass beads are very porous, they
360 offer a very conservative test for chamber induced anomalies. The high porosity offers very little
361 resistance to mass flow of CO_2 into or out of the beads, so small pressure artifacts from the
362 chamber cause immediately detectible changes in CO_2 efflux.

363 Chamber measurements showed relatively good agreement with the column effluxes over
364 a wide range of efflux rates at two chamber flow rates (Figure 4). For the chamber flow rate of
365 300 mL min^{-1}, the data adhere to the 1:1 line very well at the lower efflux rates but tend to
366 underestimate at the two highest flux rates. This may be a reason to use higher flow rates when
367 CO_2 efflux is relatively high. Chamber headspace [CO_2] increases proportionally with increasing
368 efflux rates. The head space [CO_2] can easily approach two or three times that of ambient with
369 low chamber flows and high efflux rates. This affects the diffusion gradient of CO_2 to the
370 surface inside the chamber, potentially reducing the efflux rate into the chamber. High test
371 column (or soil respired) efflux rates also increase the amount of time needed for the [CO_2] in
372 the headspace to reach equilibrium. Additionally, though pressure of the chamber is equalized to
373 that of the atmosphere prior to placing the chamber on the collar, long periods for stabilizing
374 allow more time for pressure anomalies to develop that can cause errors in chamber
375 measurements.
376 Measurements of $\delta^{13}C_R$ and $\delta^{18}O_R$ show that this chamber method is also valid for
377 determining isotopic composition from soil respired CO_2 (Figure 5). The difference between
378 measured and actual $\delta^{13}C_R$ and $\delta^{18}O_R$ values are not statistically different from zero for all CO_2
379 efflux rates. At higher efflux rates, measured values of $\delta^{13}C_R$ tend to be more enriched than the
380 known value; the average difference (Table 1) of +0.08‰ for all measurements becomes
381 +0.28‰ after omitting the two measurements at the lowest column efflux rates. This holds true
382 for $\delta^{18}O$ measurements as well, while the average measured value is -0.08‰ from the test
383 column value, omitting the same two measurements changes the mean difference to +0.26‰.
384 Several factors can cause the chamber measured values of δ_R to be isotopically enriched.
385 Since the inlet gas into the chamber is medical grade compressed air, its isotopic content is

386 similar to that of ambient air, $\delta^{13}C$ = -8.46‰ and $\delta^{18}O$ = 28.1‰. The test column air was from an
387 industrial source and therefore, the CO_2 is depleted relative to the atmosphere by more than 30‰
388 for $\delta^{13}C$ and 18‰ for $\delta^{18}O$. Due to the addition of pure CO_2 as the source gas for efflux, minor
389 pressure artifacts that suppress the surface efflux could bias measured values toward atmospheric
390 levels.

391 The active mixer and baffles on either end of the chamber are intended to disrupt laminar
392 flow and aid in maintaining a well mixed chamber environment; however there is a chance that
393 inefficient mixing could create a boundary layer near the surface causing a bias towards inlet δ_R
394 values, especially at higher flow-through rates. Invasion of atmospheric CO_2 into the interspace
395 of the glass beads as well as into the inner volume of the test chamber would enrich the source
396 for column-respired CO_2. We accounted for invasion by measuring the test column interspace
397 $\delta^{13}C$ and $\delta^{18}O$ directly and correcting for the enrichment due to kinetic fractionation. These
398 interspace values could be affected by a change in diffusion gradients when the chamber is
399 placed on the column and would also be affected by mass movements of CO_2 from temperature
400 changes or pressure changes induced by the chamber.

401 The error seen in the two measurements at the lowest efflux rates (Figure 5) could be
402 caused by changes of the test column CO_2 due to diffusion of atmospheric air into the test
403 column. Prior to measurements, the column was scrubbed of CO_2 by sealing the top of the
404 column and recirculating its air through a soda-lime scrubber. After this was completed, pure
405 CO_2 gas from an industrial source was immediately introduced and had $\delta^{13}C$ = -41.3‰ and $\delta^{18}O$
406 = 3.8‰. The ambient CO_2 in the room where the testing was performed had a $\delta^{13}C$ value of
407 approximately -9‰ and $\delta^{18}O$ value of approximately 42‰, both of which are more enriched than
408 the CO_2 source for the test column so diffusion into the test column would enrich the δ values for

409 both isotopes. Since the first two chamber efflux rate measurements of the column (Figure 5,
410 two lowest efflux rates) were the first measurements conducted after scrubbing CO_2 from the
411 column, the diffusion of ambient CO_2 may not have reached equilibrium. The first two
412 measurements (Figure 5) of $\delta^{13}C_R$ (-40.0‰ and -39.8‰) and $\delta^{18}O_R$ (7.9‰ and 8.0‰
413 respectively) measured by the chamber were much closer to δ values of the source CO_2 and had a
414 high standard deviation that could be explained by the isotopic composition inside of the test
415 column changing toward the more enriched values of ambient CO_2 during these measurements.
416 Later measurements were conducted at least 3 days after scrubbing CO_2 from the column and
417 allowed sufficient time for the influence of ambient CO_2 on the column to stabilize.
418
419 *Water Addition Experiment*
420 In the field, high temporal resolution sampling of soil CO_2 efflux, $\delta^{13}C_R$ and $\delta^{18}O_R$
421 isotope values from the chamber captured dramatic shifts after the addition of water to a dry
422 (Figure 6). Prior to water addition, soil efflux was less than 1 $\mu mol\ m^{-2}\ s^{-1}$. This was consistent
423 with field measurements conducted in a nearby site using a Li-Cor 6400-09 soil chamber and is
424 typical for dry conditions during late spring in this region. Isotopic measurements of CO_2 were
425 highly variable during the pre-watering period. This variability is likely a result of both inherent
426 spatial heterogeneity as well as a measurement artifact. The differential between chamber inlet
427 and outlet [CO_2] when efflux rates were very low was small (<30 $\mu mol\ mol^{-1}$), which leads to
428 poor precision in online estimates of $\delta^{13}C$ and $\delta^{18}O$ respired from the soil surface. This is due to
429 the larger impact on δ_R values resulting from errors in δ_o and δ_i measurements when there is a
430 small difference in c_o and c_i in equation 5. For example, if the chamber c_o = 420 $\mu mol\ mol^{-1}$ and
431 c_i = 400 $\mu mol\ mol^{-1}$, a measurement error of 0.05‰ for both δ_o and δ_i changes the δ_R value by

2‰. If the CO_2 differential is raised to 50 μmol mol^{-1} (c_o = 450 and c_i = 400 μmol mol^{-1}), the same error changes δ_R by 0.8‰.

The addition of a 50 mm watering event revealed a large shift in both efflux rate and isotopic composition. On average there was a 6.9 μmol m^{-2} s^{-1} increase in CO_2 efflux; an increase of nearly 24-fold. The initial increase in CO_2 efflux could be attributed to the displacement of CO_2 in the soil from the 792 mL of water that were added; however, we saw only one soil collar that exhibited a pulse of CO_2 before returning to a stable, elevated flux (Figure 6 panel A). Based on the displacement of 792 mL of soil gas with an estimated [CO_2] of 2000 μmol mol^{-1}, the increase in soil CO_2 efflux cannot be explained solely by displacement (Figure 7). All soil collar measurements showed a sustained increase in CO_2 efflux until measurements were terminated, at least 35 minutes after water addition.

The addition of water to the chamber also produced an average shift of -5.0‰ for $\delta^{13}C_R$. We do not know what caused the shift in $\delta^{13}C_R$ but we speculate that is due to an increase in heterotrophic activity as well as transient diffusive effect due to non-steady state conditions (Moyes 2008, Risk and Kellman 2008). Since the soil at this site is very low in carbonates, we do not expect any contribution from carbonates to affect efflux $\delta^{13}C$ values. There were several large *Juniperus monosperma* in the sampling site so there could have been some respiratory response from the root system; however, the *Juniperus* canopies are unlikely to have responded with increased photosynthesis because the water was over a small area and the response happened immediately after watering. Most likely, the addition of water initiated a respiratory response from heterotrophic organisms in the soil that were inactive under dry conditions, prompting a shift in the substrates used for decomposition and hence a shift in the isotopic composition of respired CO_2 (Xu et al. 2004). Isotopic measurements from roots and leaves of

455 plants from the site (*Juniperus monospera, Bouteloua gracilis, Gutierrezia sarothrae, Poa*
456 *fendleriana*) have $\delta^{13}C$ values of approximately -22.3‰, similar to values measured by the
457 chamber before watering (Figure 6 panel B). After watering, chamber $\delta^{13}C$ measurements are
458 consistent with bulk soil $\delta^{13}C$ of -29‰, indicating a shift in the source CO_2 for respiration.
459 The benefit of using high frequency measurements is apparent here in that the
460 measurement rate of one measurement every two minutes captures the rapid change in soil CO_2
461 efflux and isotopic composition after the pulse watering event (Figure 6). Sampling on a lower
462 frequency time scale of hours or days would likely not capture the change seen here with
463 sufficient resolution to determine the time after watering in which a response is detected and the
464 magnitude of the changes at their maximums. It is conceivable that once-daily measurements
465 would not detect the majority of the response evoked by short lived rain events, particularly in
466 the arid ecosystems of the southwestern United States that are subject to short but intense pulse
467 rain events. The usefulness of soil CO_2 efflux and isotope measurements is drastically increased
468 by higher frequency measurement intervals.
469 The $\delta^{18}O_R$ value dropped by -55‰ after water was added within the soil collar, from
470 80.3‰ to 25.3‰. This was expected since liquid water exchanges ^{18}O atoms with CO_2 and the
471 water we applied had a $\delta^{18}O$ of -10.8‰, which should impart a $\delta^{18}O$ value of 22.5‰ onto soil
472 CO_2 in the vicinity of the water (Mook et al. 1974). Mass spectrometer analysis of water
473 extracted from the soil after watering shows water in the top 0 – 20 mm of soil have
474 approximately the same $\delta^{18}O$ as the water that was used, with soil water becoming progressively
475 enriched with depth. Prior to watering, extracted soil water values were +5‰ to -2‰, indicating
476 that the $\delta^{18}O$ of the soil water was enriched due to evaporation. A model was used to predict the
477 $\delta^{18}O_R$ of CO_2 in isotopic equilibrium with the extracted soil water (Figure 8). For the dry soils,

the model predicts much lower $\delta^{18}O_R$ values than what was seen with the soil chamber. However, nightly, ecosystem-scale Keeling plots generated from data collected with the *TDL* at this site gave intercepts between 54‰ and 68‰, closer to the soil chamber data. It is possible that the highly enriched $\delta^{18}O$ of respired CO_2 measured prior to watering results from a high ratio of invasion of soil "respiration" *per se* during dry conditions.

Conclusion

Our data show that the soil chamber- TDL system was capable of measuring soil efflux and isotopic composition effectively and with high frequency. When the soil chamber was used with a test column where efflux rate and isotopic composition were tightly controlled, chamber measurements closely matched the column efflux rate and had an average difference of -0.08‰ for $\delta^{13}C_R$ of -0.08‰ for $\delta^{18}O_R$. We found no statistical difference between measured and test column values for both fluxes and isotopes. Our results confirm prior observations that careful regulation of pressure artifacts and consideration of flow rates relative to CO_2 efflux rates is warranted. The chamber-TDL system also proved capable of high temporal resolution sampling of effluxes and isotope signals from transient responses to *in situ* watering events in a field setting.

Acknowledgements

We thank Will Pockman for help in determining the course of this research and for helpful comments on the draft manuscript. Thanks to Clif Meyer, Dave Bowling, and Dan Breeker for helpful input and technical assistance. Thanks to Steve Sargent for help with laser spectroscopy. Thanks also to the LDRD program at Los Alamos National Laboratory for funding and the UNM

501 Biology department for support.

502

503 **Citations**

504 Amundson R, Stern L, Baisden T, Wang Y (1998) The isotopic composition of soil and soil-
505 respired CO2. *Geoderma,* **82**, 83-114.

506 Barbour MM, Farquhar GD, Hanson DT, Bickford CP, Powers HH, McDowell NG (2007) A
507 new measurement technique reveals temporal variation in delta18o of leaf-respired CO2.
508 *Plant, Cell & Environment,* **30**, 456.

509 Battle M, Bender ML, Tans PP, White JWC, Ellis JT, Conway T, Francey RJ (2000) Global
510 carbon sinks and their variability inferred from atmospheric O-2 and delta C-13. *Science,*
511 **287**, 2467-2470.

512 Bender MM (1971) Variations in C-13/C-12 ratios of plants in relation to pathway of
513 photosynthetic carbon dioxide fixation. *Phytochemistry,* **10**, 1239.

514 Bowling D, Sargent S, Tanner B, Ehleringer J (2003) Tunable diode laser absorption
515 spectroscopy for stable isotope studies of ecosystem–atmosphere CO2 exchange.
516 *Agricultural and Forest Meteorology,* **118**, 1.

517 Bowling DR, Burns SP, Conway TJ, Monson RK, White JWC (2005) Extensive observations of
518 CO2 carbon isotope content in and above a high-elevation subalpine forest. *Global*
519 *Biogeochemical Cycles,* **19**, GB3023.

520 Cerling TE (1984) The stable isotopic compsition of modern soil carbonate and its relationship to
521 climate. *Earth and Planetary Science Letters,* **71**, 229-240.

522 Cerling TE, Solomon DK, Quade J, Bowman JR (1991) On the isotopic compositon of carbon in
523 soil carbon dioxide. *Geochimica et Cosmochimica Acta,* **55**, 3403-3406.

524 Ciais P, Tans PP, White JWC, *et al.* (1995) Partitioning of ocean and land uptake of CO2 as
525 inferred by delta-C-13 measurements from the noaa climate monitoring and diagnostics
526 laboratory global air sampling network. *Journal of Geophysical Research-Atmospheres,*
527 **100**, 5051-5070.
528 Davidson EA, Savage K, Verchot LV, Navarro R (2002) Minimizing artifacts and biases in
529 chamber-based measurements of soil respiration. *Agricultural and Forest Meteorology,*
530 **113**, 21-37.
531 Ehleringer JR, Buchmann N, Flanagan LB (2000) Carbon isotope ratios in belowground carbon
532 cycle processes. *Ecological Applications,* **10**, 412-422.
533 Ekblad A, Hogberg P (2000) Analysis of delta C-13 of CO2 distinguishes between microbial
534 respiration of added C-4-sucrose and other soil respiration in a C-3-ecosystem. *Plant and*
535 *Soil,* **219**, 197-209.
536 Evans JR, Sharkey TD, Berry JA, Farquhar GD (1986) Carbon isotope discrimination measured
537 concurrently with gas exchange to investigate carbon dioxide diffusion in leaves of
538 higher plants. *Australian Journal of Plant Physiology,* **13**, 281-292.
539 Fang C, Moncrieff JB (1996) An improved dynamic chamber technique for measuring CO2
540 efflux from the surface of soil. *Functional Ecology,* **10**, 297-305.
541 Farquhar GD, Lloyd J, Taylor JA, *et al.* (1993) Vegetation effects on the isotope composition of
542 oxygen in atmospheric CO2. *Nature,* **363**, 439-442.
543 Fung I, Field CB, Berry JA, *et al.* (1997) Carbon 13 exchanges between the atmosphere and
544 biosphere. *Global Biogeochemical Cycles,* **11**, 507-533.

545 Griffis TJ, Lee X, Baker JM, Sargent SD, King JY (2005) Feasibility of quantifying ecosystem-
546 atmosphere (COO)-O-18-O-16 exchange using laser spectroscopy and the flux-gradient
547 method. *Agricultural and Forest Meteorology,* **135**, 44-60.
548 Law BE, Baldocchi DD, Anthoni PM (1999) Below-canopy and soil CO2 fluxes in a ponderosa
549 pine forest. *Agricultural and Forest Meteorology,* **94**, 171-188.
550 Lund CP, Riley WJ, Pierce LL, Field CB (1999) The effects of chamber pressurization on soil-
551 surface CO2 flux and the implications for nee measurements under elevated CO2. *Global*
552 *Change Biology,* **5**, 269-281.
553 McDowell NG, Bowling DR, Bond BJ, Irvine J, Law BE, Anthoni P, Ehleringer JR (2004)
554 Response of the carbon isotopic content of ecosystem, leaf, and soil respiration to
555 meteorological and physiological driving factors in a pinus ponderosa ecosystem. *Global*
556 *Biogeochemical Cycles,* **18**, GB1013.
557 McDowell NG, Baldocchi DD, Barbour MM, *et al.*,(2008) Understanding the stable isotope
558 composition of biosphere-atmosphere CO2 exchange. *EOS,* **89**, 94-95.
559 Miller JB, Yakir D, White JWC, Tans PP (1999) Measurement of O-18/O-16 in the soil-
560 atmosphere CO2 flux. *Global Biogeochemical Cycles,* **13**, 761-774.
561 Miller JB, Tans PP, White JWC, Conway TJ, Vaughn BW (2003) The atmospheric signal of
562 terrestrial carbon isotopic discrimination and its implication for partitioning carbon
563 fluxes. *Tellus. Series B, Chemical and Physical Meteorology,* **55B**, 197-206.
564 Mook WG, Bommerson JC, Staverman WH (1974) Carbon isotope fractionation between
565 dissolved bicarbonate and gaseous carbon dioxide. *Earth and Planetary Science Letters,*
566 **22**, 169-176.
567 Moyes AB (2008) *Personal communication*

568 Raich JW, Schlesinger WH (1992) The global carbon-dioxide flux in soil respiration and its
569 relationship to the vegetation and climate. *Tellus. Series B, Chemical and Physical*
570 *Meteorology,* **44**, 81-99.
571 Randerson JT, Chapin FS, Harden JW, Neff JC, Harmon ME (2002a) Net ecosystem production:
572 A comprehensive measure of net carbon accumulation by ecosystems. *Ecological*
573 *Applications,* **12**, 937-947.
574 Randerson JT, Still CJ, Balle JJ, *et al.* (2002b) Carbon isotope discrimination of arctic and boreal
575 biomes inferred from remote atmospheric measurements and a biosphere-atmosphere
576 model - art. No. 1028. *Global Biogeochemical Cycles,* **16**, 1028-1028.
577 Rayment MB, Jarvis PG (1997) An improved open chamber system for measuring soil CO2
578 effluxes in the field. *Journal of Geophysical Research,* **102**, 28779-28784.
579 Risk D, Kellman L (2008) Isotopic fractionation in non-equilibrium diffusive environments.
580 *Geophysical Research Letters,* **35**, L02403
581 Tans PP (1998) Oxygen isotopic equilibrium between carbon dioxide and water in soils. *Tellus.*
582 *Series B, Chemical and Physical Meteorology* **50**, 163-178.
583 Widen B, Lindroth A (2003) A calibration system for soil carbon dioxide efflux measurement
584 chambers: Description and application. *Soil Science Society of America Journal,* **67**, 327-
585 334.
586 Xu LK, Baldocchi DD, Tang JW (2004) How soil moisture, rain pulses, and growth alter the
587 response of ecosystem respiration to temperature. *Global Biogeochemical Cycles,* **18**,
588

589 **Table 1.** Chamber measurements of CO_2 efflux, $\delta^{13}C_R$, and $\delta^{18}O_R$ (mean + SD) from a test
590 column of dry glass beads, Known values for respired CO_2 were $\delta^{13}C$ = -39.0±0.3‰ and $\delta^{18}O_R$
591 = 9.7±0.3‰. Paired t-test at the 95% confidence level across all chamber flow rates and
592 analyzed for each flow rate gives no significant difference in the chamber mean value and known
593 value of δ_R. All flow rates: $\delta^{13}C_R$ = -38.9±0.6‰ (p = 0.66) and $\delta^{18}O_R$ = 9.6±1.1‰ (p = 0.81).
594 300 mL min^{-1}: $\delta^{13}C_R$ = -39.3±0.6‰ (p = 0.40), $\delta^{18}O_R$ = 9.0±1.0‰ (p = 0.21). 500 mL min^{-1}:
595 $\delta^{13}C_R$ = -38.7±0.5‰ (p = 0.13), $\delta^{18}O_R$ = 10.1±0.9‰ (p = 0.34)

Chamber flow rate ($\mu mol\ s^{-1}$)	Chamber CO_2 efflux ($\mu mol\ m^2\ s^{-1}$)	S.D. of efflux	Column CO_2 efflux ($\mu mol\ m^2\ s^{-1}$)	Chamber $\delta^{13}C_R$ (‰)	S.D. of $\delta^{13}C_R$	Difference from 39.0‰	Chamber $\delta^{18}O_R$ (‰)	S.D. of $\delta^{18}O_R$	Difference from 9.7‰
300	1.17	0.04	0.94	-40.03	1.34	0.13	7.92	2.26	1.78
300	1.75	0.19	1.83	-39.77	1.60	-0.13	8.00	2.42	1.70
300	2.97	0.28	2.71	-38.43	1.19	-1.47	10.35	1.62	-0.65
300	3.24	0.23	3.86	-39.06	0.60	-0.84	9.39	0.92	0.31
300	3.61	0.27	4.59	-39.06	0.79	-0.84	9.38	1.17	0.32
500	2.60	0.08	2.62	-39.59	1.02	-0.31	8.49	1.34	1.21
500	3.29	0.31	3.35	-38.90	0.72	-1.00	9.60	1.58	0.10
500	4.87	0.27	4.15	-38.11	0.57	-1.79	11.35	0.92	-1.65
500	5.03	0.17	5.08	-38.69	0.48	-1.21	10.05	0.78	-0.35
500	5.41	0.40	5.82	-38.74	0.63	-1.16	9.81	1.05	-0.11
500	7.06	0.53	6.66	-38.13	0.52	-1.77	10.94	0.85	-1.24
500	7.11	0.22	7.51	-38.51	0.54	-1.39	10.17	0.78	-0.47

596

Table 2. CO_2 efflux, $\delta^{13}C_R$, and $\delta^{18}O_R$ (mean + SD) from a dry grassland, before and after addition of 50 mm of irrigation

Watering	Collar #	Soil CO_2 Efflux ($\mu mol\ m^2 s^{-1}$)	S.D. of Efflux ($\mu mol\ m^2 s^{-1}$)	$\delta^{13}C_R$ (‰)	S.D. of $\delta^{13}C_R$ (‰)	$\delta^{18}O_R$ (‰)	S.D. of $\delta^{18}O_R$ (‰)	SWC 0-10 cm (%)
Pre-water addition	1	0.3	0.05	-22.9	2.36	70.4	4.82	
	2	0.1	0.02	-23.0	4.51	82.9	10.01	3.6
	3	0.3	0.05	-19.3	3.12	70.7	9.73	2.0
	4	0.2	0.06	-18.3	3.00	85.9	5.59	2.8
	5	0.7	0.06	-22.6	2.40	85.6	5.45	2.3
	6	0.2	0.06	-17.6	2.50	86.3	10.40	3.3
Post-water addition	1	4.2	0.2	-27.3	1.4	22.2	2.3	-
	2	3.1	0.3	-27.0	0.6	23.7	0.9	13.9
	3	10.2	0.3	-24.6	0.5	26.5	1.5	11.7
	4	5.9	1.2	-26.6	0.9	23.9	1.2	11.8
	5	9.8	0.1	-23.0	0.3	30.0	0.9	15.2
	6	10.1	0.8	-25.1	0.5	25.8	0.6	18.2

Figure 1. Dynamic soil chamber and gas sampling system using mass flow controllers connected to a *TDL* analysis system. Flow from a compressed cylinder of air is controlled by a MFC and a tee that acts as a pressure bypass. The air is sub-sampled by the *TDL* before and after it enters the chamber. A mass flow controller regulates the flow out of the chamber to the pump.

Figure 2. The constant-flux test column system maintains a set concentration of CO_2 below the dry glass beads (soil substrate) in order to both generate and precisely measure stable CO_2 fluxes through the substrate.

Figure 3. Comparison of two independent CO_2 efflux measurements: calculated using the *TDL* measurements and an IRGA (LI-840). In both cases the chamber CO_2 efflux rate ($\mu mol\ m^{-2}s^{-1}$) was calculated based on the difference in CO_2 concentration between the air entering and the air exiting the chamber (equation 1). A 1:1 line (dashed) is shown for comparison. Least means squared regression equation: $y = 0.99x - 0.02$, $R^2 = 0.99$.

Figure 4. Comparison of TDL-based chamber measurements of CO_2 efflux to known CO_2 efflux from the test column. The test column system produced known efflux rates through manipulation of headspace [CO_2] below the porous medium on which the chamber rested. Flow-through rates of gas through chamber headspace were varied in order to maintain an adequate differential between sample and reference CO_2 concentrations; flow-through rates of 300 mL min^{-1} (closed symbols) and 500 mL min^{-1} (open symbols) are shown. A 1:1 line (dashed) is shown for comparison.

Figure 5. Tests of soil chamber measurements of A) $\delta^{13}C_R$ and B) $\delta^{18}O_R$ using constant isotopic sources across a range of CO_2 efflux rates. Dashed lines represent actual isotopic (δ_m) values found by sampling the test column headspace and correction for diffusive fractionation ($\delta^{13}C_R = \delta_m - 4.4‰$ and $\delta^{18}O_R = \delta_m - 8.8‰$). Through flow rates of 300 mL min^{-1} (closed symbols) and 500 mL min^{-1} (open symbols) are shown.

Figure 6. Field measurements of A) soil CO_2 efflux rates, B) respired $\delta^{13}C$ and C) $\delta^{18}O$ from six locations in a piñon-juniper woodland. A 50 mm rain event was simulated through application of 183 mL of water through a port within the chamber (time = 0 minutes). (Both $\delta^{13}C$ and $\delta^{18}O$ are highly variable prior to watering, resulting from the mixing model's sensitivity to the small differential between incoming and outgoing [CO_2] concentration caused by the near-zero soil efflux rate. Water addition produces a precipitous increase in soil CO_2 efflux and a shift to more negative $\delta^{13}C_R$ values and the expected decline in $\delta^{18}O_R$ as the CO_2 picks up the signal of the water (-10.1‰).

Figure 7. Bold line shows contribution to CO_2 efflux that could occur from displacing soil gas during the water addition. Gray lines show chamber CO_2 efflux rates for comparison. Displacement equivalent to 792 mL of soil gas (from water volume) with 1000 µmol mol^{-1} [CO_2] is equivalent to 25 µmol of CO_2 which is the area under the bold curve.

Figure 8. A) Modeled $\delta^{18}O$ of soil CO_2 before (Δ) and after ($\blacktriangle$) the addition of water. B) Measured gravimetric water content collected beside the chambers before ($\bullet$) and under the chamber after ($\circ$) the addition of water.

650
651 **Figure 1.**

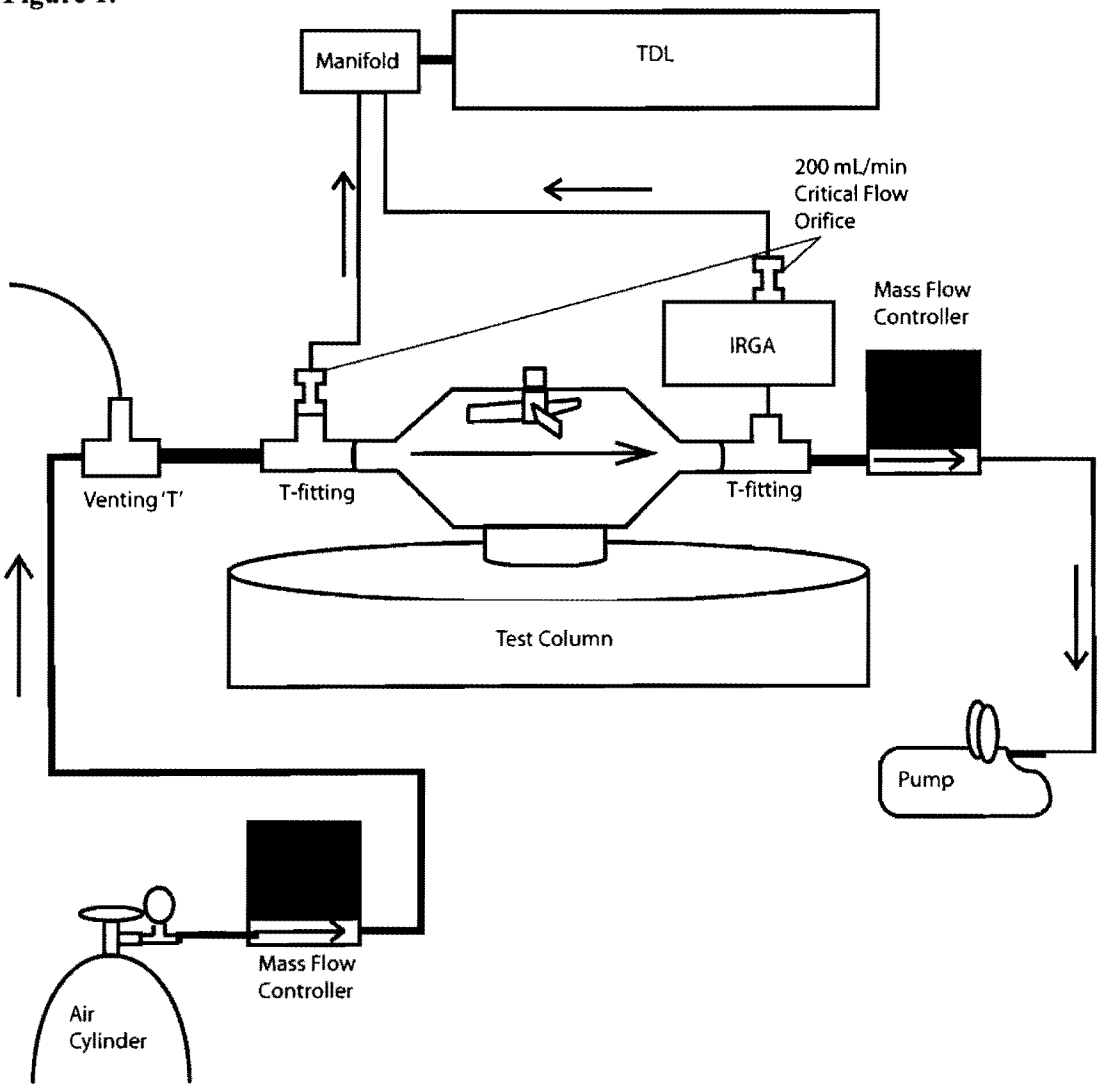

652

653 **Figure 2.**

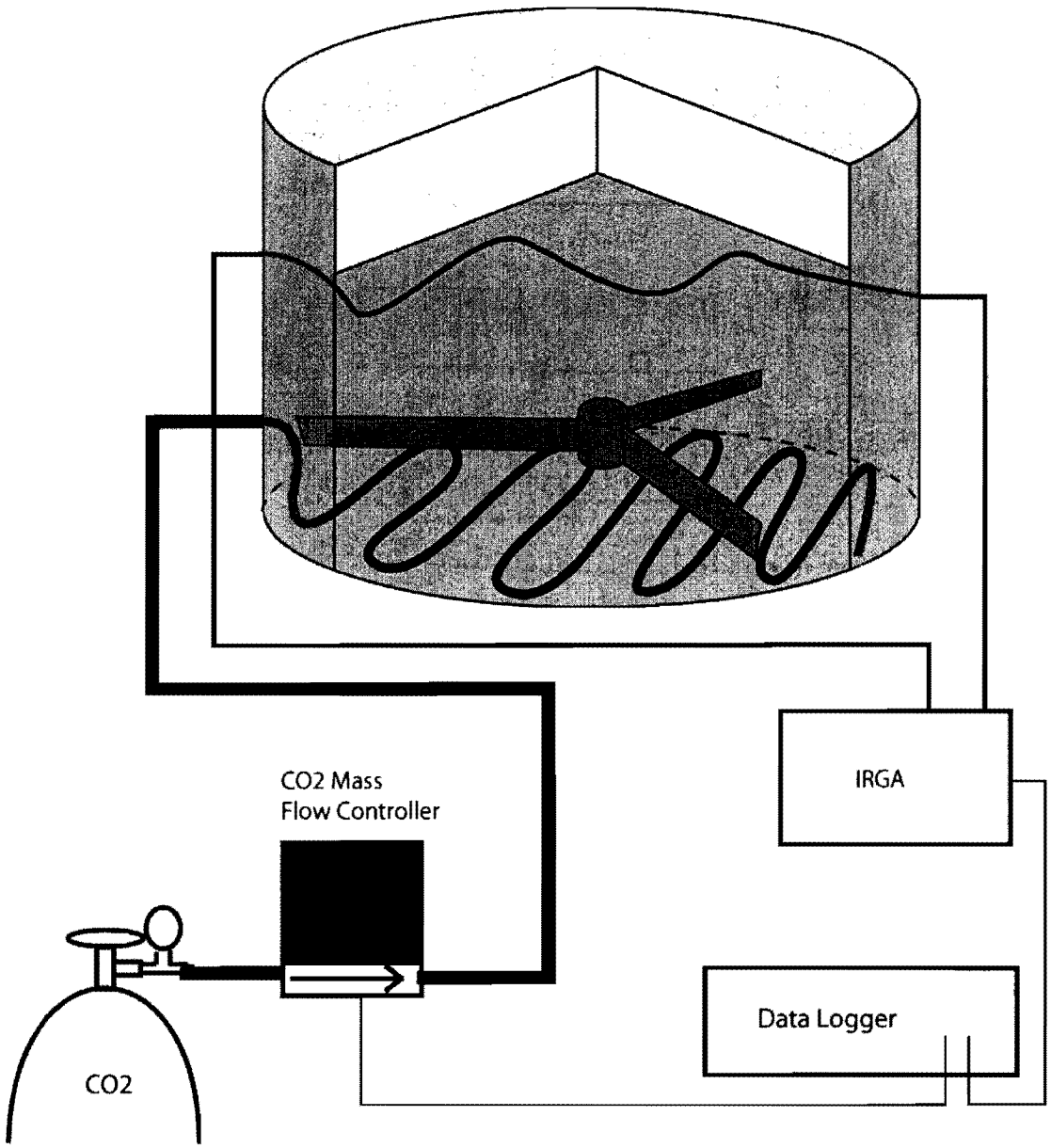

654
655
656

657
658 **Figure 3.**

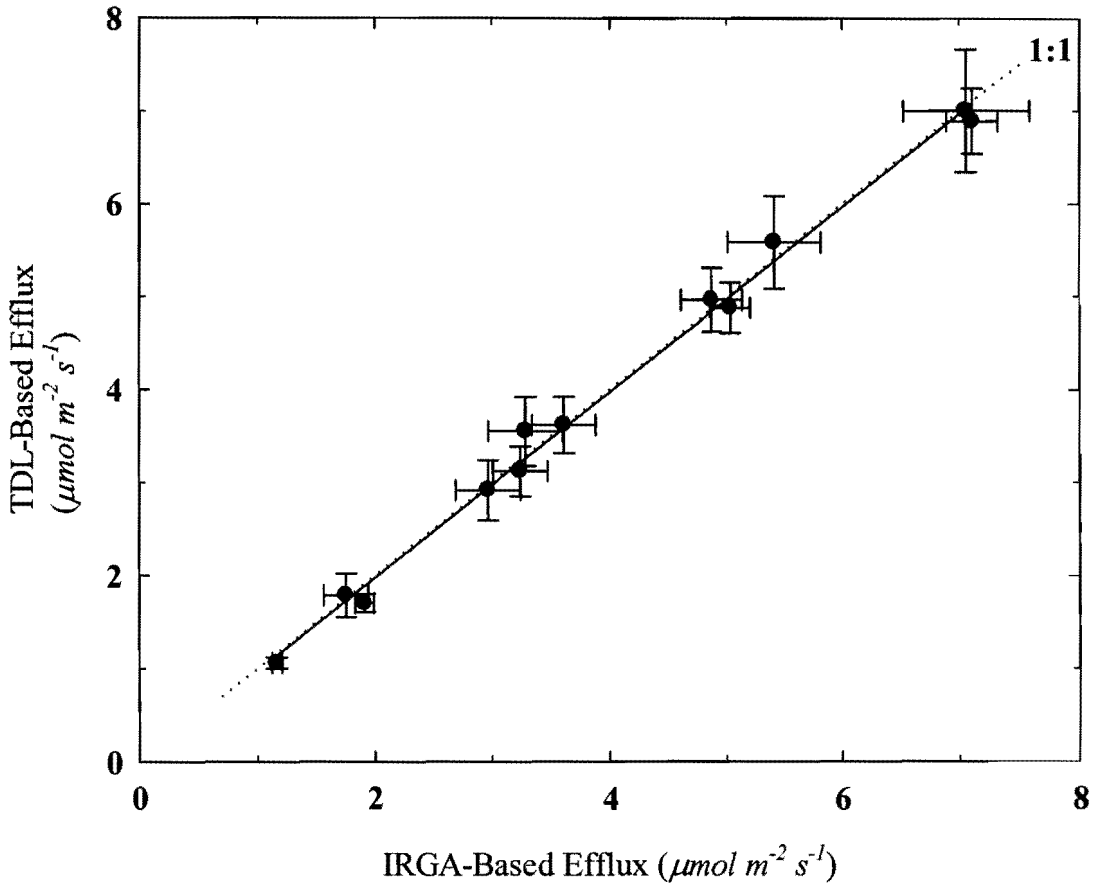

659
660
661

662
663 **Figure 4.**

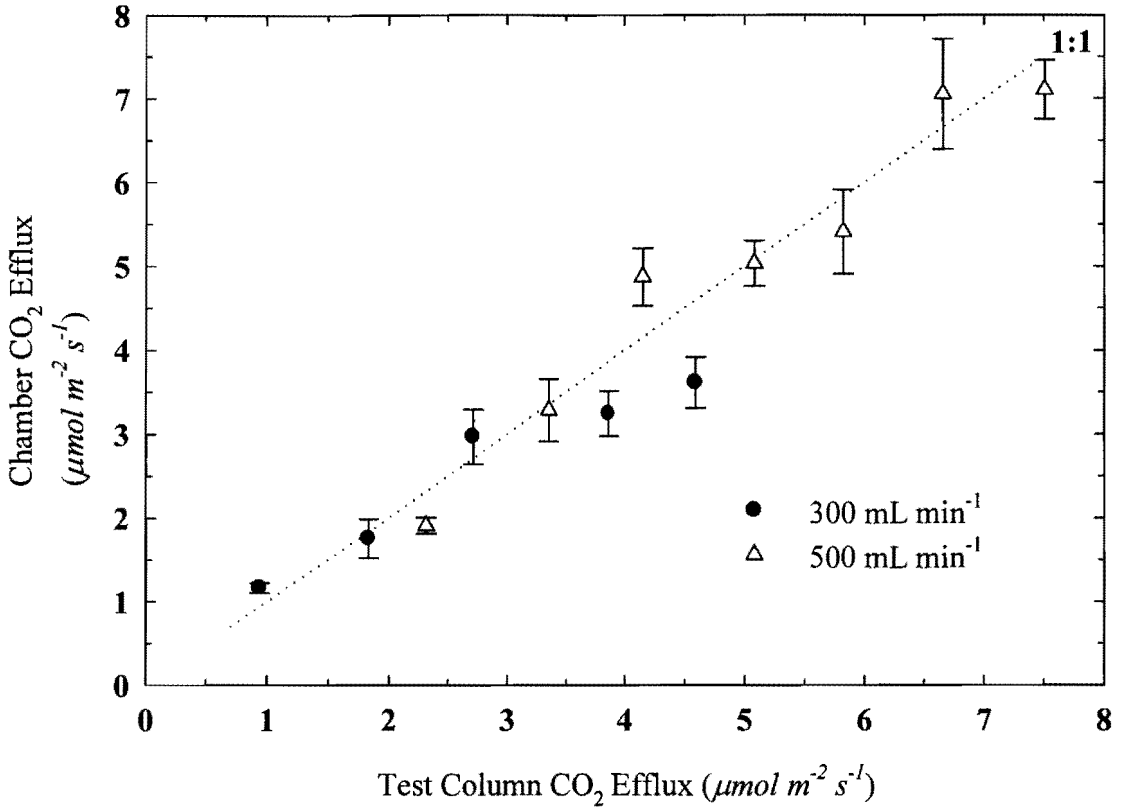

664

665
666

Figure 5.

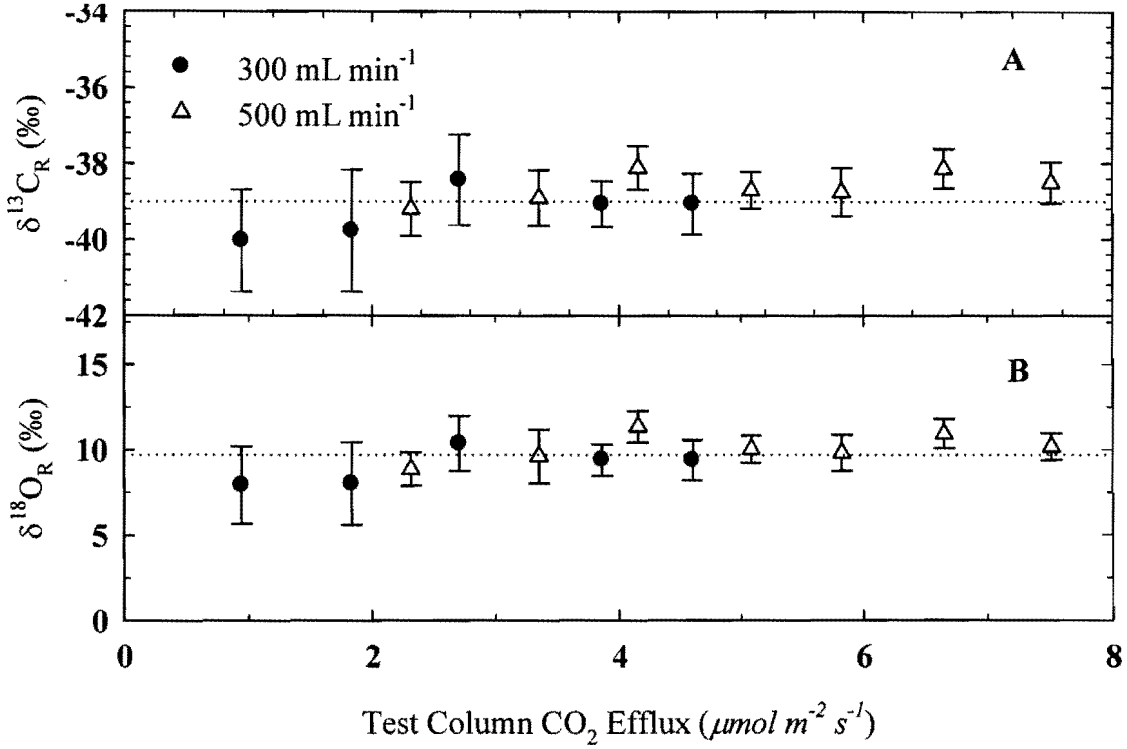

667
668

669
670 **Figure 6.**

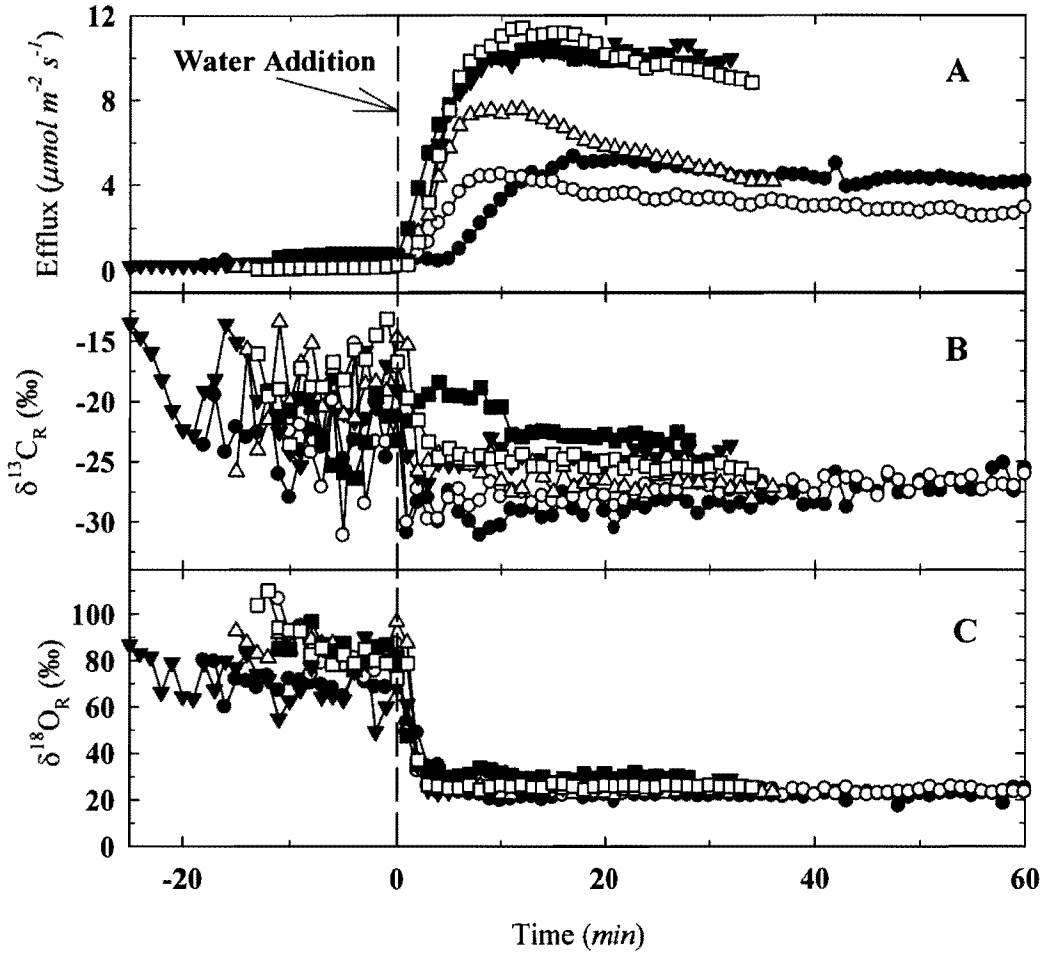

671

672 **Figure 7.**

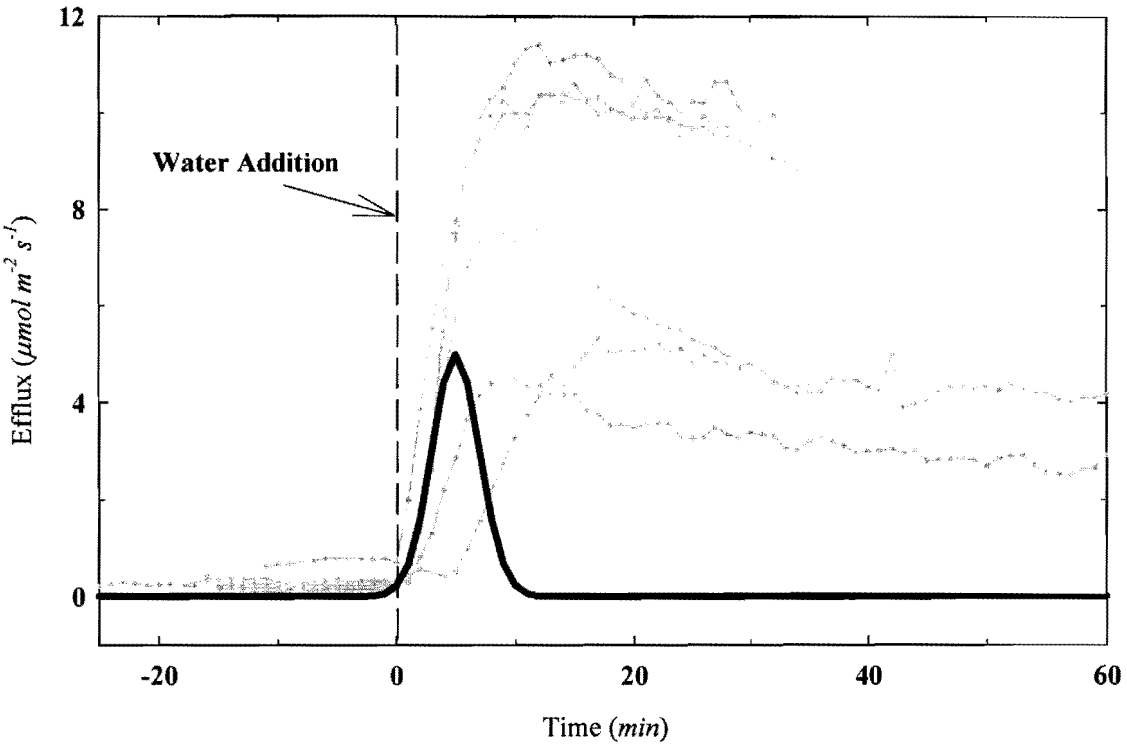

673

674
675 **Figure 8.**
676

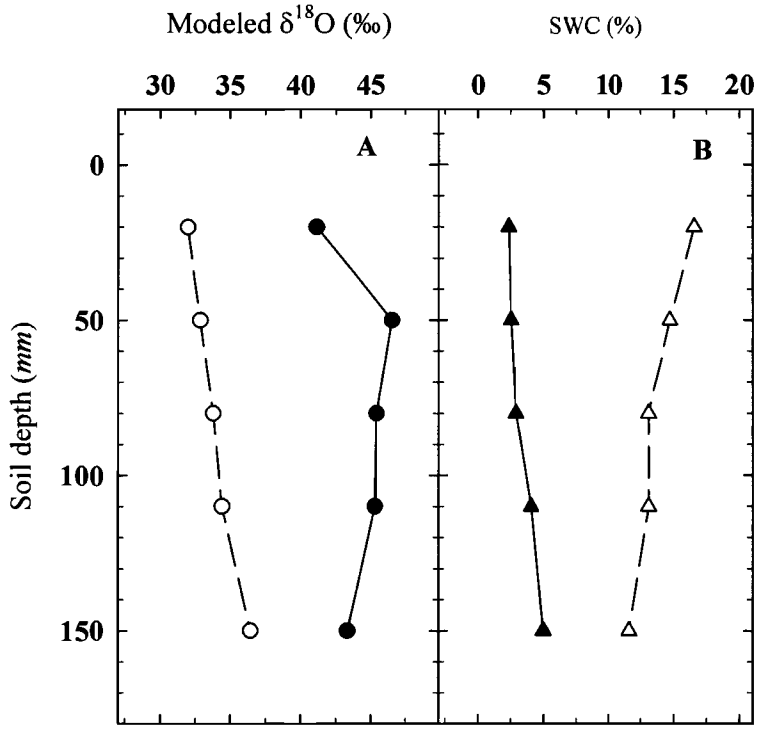

677